Colloid Polym Sci 276:753–768 (1998)

ORIGINAL CONTRIBUTION

L.V. Zherenkova
D.A. Mologin
P.G. Khalatur
A.R. Khokhlov

Interaction between small colloidal particles and polymer chains in a semidilute solution: Monte Carlo simulation

Received: 4 August 1997
Accepted: 16 April 1998

L.V. Zherenkova · D.A. Mologin
P.G. Khalatur (✉)
Department of Physical Chemistry
Tver State University
Tver 170002
Russia

A.R. Khokhlov
Physics Department
Moscow State University
Moscow 117234
Russia

Abstract Interaction between flexible-chain polymers and small (nanometric) colloidal particles is studied by Monte Carlo simulation using two-dimensional and three-dimensional lattice models. Spatial distribution of colloidal particles and conformational characteristics of chains in a semidilute solution are considered as a function of the segment adsorption energy, ε. When adsorption is sufficiently strong, it induces effective attraction of polymer segments, which results in contraction of macromolecular coils. The strongly adsorbing polymer chains affect the equilibrium spatial distribution of the colloidal particles. The average size of colloidal aggregates $\langle m \rangle$ exhibits a nontrivial behavior: with ε increasing, the value of $\langle m \rangle$ first decreases and then begins to grow. The adsorption *polycomplex* formed at strong adsorption exhibits a mesoscopic scale of structural heterogeneity. The results of computer simulations are in a good agreement with predictions of the analytic theory [P.G. Khalatur, L.V. Zherenkova and A.R. Khokhlov (1997) J Phys II (France) 7:543] based on the integral RISM equation technique.

Key words Colloids – macromolecules – solution – interaction – computer simulation

Introduction

A wide use of polymers as stabilizers of colloid systems (sols, dispersions, microemulsions, micellar solutions, etc.) is one of the important trends in chemical technology. First of all this is due to the fact that even very small polymer additives can have a crucial effect on the aggregation and kinetic stability of colloidal particles [1, 2]. Polymer-containing colloidal dispersions may be used in order to control or modify flow properties of liquids; depending on the concentrations of the polymer and the particles as well as the interaction between them, the dispersions may be shear thickening or shear thinning [3, 4]. New precision methods (in particular, small-angle neutron scattering) allow one to observe rather exotic structures which emerge due to the adsorption of macromolecules on the surface of supersmall (nanometric) particles [5–13]. These structures are controlled by a balance of forces of the electrostatic interparticle repulsion and the effective attraction which is induced by polymer chains sorbed on the particles.

In the theory of polymer-containing disperse systems, we can conventionally distinguish two large classes of problems. One of these classes includes the problems of classical chemistry of colloids and physical chemistry of surface phenomena, e.g., description of the surface electrical phenomena [2]. The other class of problems is in closer contact with traditional fields of polymer physics. In treating these problems, the details of interaction between colloidal particles usually are out of consideration and the attention is focused on the pure "polymer contribution", which depends on the concentration of dissolved macromolecules, the character of their interaction with the particles, thermodynamic properties of the solvent, etc. This

approach is adopted in a series of theoretical works [14–44] based on the mean-field approximation or the scaling concept. The most general results were obtained by Klimov and Khokhlov in ref. [44]. In this work, the free energy of the system, $\Delta\mathcal{F}$, was written as a sum of different contributions, using the scaling estimates. As is shown in ref. [44], when particles are fixed in space, the polymer chain takes a strongly elongated conformation. In contrast to this, when adsorption occurs on moving particles, the chain assumes conformations similar to a typical conformation of a free chain in solution.

In past few years, there have been several investigations of a polymer-containing colloid system on the basis of integral equation theory [45–47]. Shaw and Thirumalaj [45] developed a statistical–mechanical theory for a system of one free polymer chain in a colloidal solution consisting of large hard-sphere particles. The polymer-colloid site–site radial distribution function was found for the simplest athermal regime, in the limit of infinitely low polymer volume fraction. Formerly, the structure of single polymer chains in random fields of obstacles was studied using a path-integral formalism [48–50]. An analogous problem was considered by Khokhlov et al. [51, 52], who calculated the partition function of a random-walk polymer chain in an array of obstacles. The interaction between hard spheres in solutions containing flexible polymer chains was studied by Yethiraj et al. [46] using the polymer-RISM (PRISM) integral equation formalism of Curro and Schweizer [53, 54]. The polymer molecules were modeled as short freely jointed chains of hard spheres. In the limit as the colloidal solution becomes infinitely diluted, the effective potential (or potential of mean force) between two hard-sphere colloidal particles immersed in a polymer solution was found.

Recently, a microscopic theory of the mixtures of adsorbing macromolecules and small colloidal particles in a common solvent has been developed on the basis of the integral RISM equation technique [47]. This theory has been used for a study of interaction between flexible polymer chains and particles, aggregation processes, and properties of structures formed under equilibrium conditions. We summarize the results of the calculations [47] in Fig. 1, which gives a schematic representation of the diagram of states of the polymer-containing colloid system in the coordinates: temperature–polymer volume fraction (density of colloidal particles is assumed to be fixed). On the dotted lines in the diagram, the reduced compressibility χ^* of the subsystem of colloidal particles is the same as for the "ideal gas" of the particles (i.e., $\chi^* = 1$). In the region A, which lies between the upper and lower dotted curves, we have $\chi^* < 1$. In two regions B, one has $\chi^* > 1$. In the subregion S, the conditions of the increased stability of the dispersion are realized. Here, the compressibility is

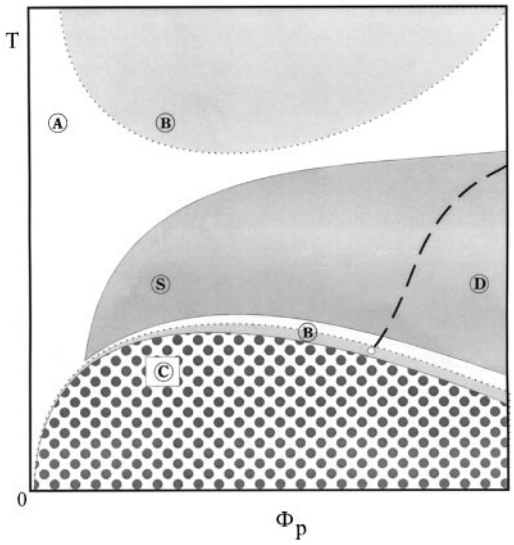

Fig. 1 Schematic state diagram of the subsystem of colloidal particles in the coordinates: temperature–polymer volume fraction [47]. The density of colloidal particles is fixed

considerably lower, as compared to the system of individual particles at the same density, i.e., stable adsorption complexes are formed because of binding together chains and particles. In the region C, intensive aggregation of particles occurs. This is due to their effective attraction mediated by strong adsorption of chains. In this case, a singularity of χ^* takes place, i.e., $\chi^* \to \infty$. The dashed line defines the region D, where the formation of quasiregular structures with periodic alternating of particles and polymer segments is observed.

Unfortunately, the above-mentioned analytic approaches suffer the drawback that the class of allowed molecular models is inevitably oversimplified. In addition, the analytic theories are not well suited to deal with situations when adsorption effects are extremely strong. In such a situation direct computer simulations of the type to be presented here can be helpful by providing numerically exact data on well-defined models, thus allowing an unambiguous test of theoretical approaches. This technique is also useful in obtaining information on various quantities that cannot be easily measured in the experiment. Here we describe a computer simulation carried out using the Monte Carlo method. This approach has been used to study the polymer-containing colloid systems [55–57] (for review see ref. [58]). Dickinson and coworkers performed Brownian dynamics simulations of the systems of multi-subunit deformable particles [59, 60]. In particular, they calculated average aggregate sizes and the corresponding equilibrium size distribution functions as a function of the site–site interaction and the strength of adhesion [59].

In the present work, we are mainly interested in the following general questions. (1) How does the adsorbing polymer component affect the interaction and spatial distribution of the small colloidal particles? (2) What is the effect of the adsorbed particles on the conformation of macromolecules? To answer these questions we carry out the Monte Carlo simulation of two- and three-dimensional systems of the type "polymer chains + colloidal particles".

In the two-dimensional (2d) case, the properties of the model binary system consisting of polymer chains and colloidal particles are compared to the corresponding properties of two reference one-component systems, one of which contains only small colloidal particles, and the other, only polymer chains. The calculations are preformed by Monte Carlo simulation for a lattice model. There are several reasons for the choice of such a "primitive" model. First, we are going to find only the most general regularities but not the detailed characteristics of some real system. Second, we can expect that the specific features of the model used (in particular, that it is discrete and two-dimensional) would not influence the basic conclusions, because we are going to compare the three systems under the same conditions. Third, the prior consideration [57] and the experimental data [5–13] indicate that the characteristic sizes of structural heterogeneities formed must be too large from the point of view of the computer resources and their observation in a three-dimensional system must be problematic due to technical reasons. For the three-dimensional (3d) system we use a lattice model as well. The second objective of our study is to carry out the comparison of theoretical predictions [47] obtained for various absorption regimes (see Fig. 1) with the results of simulations.

The organization of this paper is as follows. We first describe the two-dimensional (2d) and three-dimensional (3d) lattice models used in the present study as well as the simulation technique, utilizing the Monte Carlo method. The numerical results of these simulations are then reported in the next section. The study is concluded with a discussion of the results and their comparison with available theoretical predictions presented in ref. [47].

Models and method of computation

The two-dimensional system

As is known [61, 58], application of conventional lattice models to the study of polymer systems at high densities or in the case of strong intermolecular interactions meets considerable difficulties, especially in the case of two-dimensional systems. Therefore, we use a special model that is the so-called bond-fluctuation model (BFM) [62, 63]. The key assumption of this model is that the bond lengths between subsequent segments are not fixed but can vary (fluctuate) in a certain interval. Like in the standard lattice models [58], in BFM, occupancy of lattice sites by more than one monomeric unit is forbidden. In addition to this, there is an additional constraint. Each monomeric unit not only occupies one lattice site but does not allow other monomers to occupy the nearest lattice sites (i.e., those at a distance of the lattice unit σ) and the nearest diagonal sites (at a distance of $2^{1/2}\sigma$) as well. Chain configurations evolve in the following way. A randomly chosen monomeric unit makes an attempt to displace to one of the eight nearest lattice sites (i.e., those at a distance of σ or $2^{1/2}\sigma$) chosen with equal probability. However, if this site is occupied or the chain connectivity constraint is not satisfied, the attempt is rejected and the monomer is left at its old site. Apparently, under the conditions described above, the minimum bond length is two lattice units. The maximum bond length of $13^{1/2}\sigma$ is chosen from geometric considerations. Apparently, at a larger maximum bond length, the chains are able to pass through each other and possess a phantom topology. Note that in the model described the artifacts typical to standard lattice algorithms are absent (in particular, the well-known nonergodicity problem [61, 58] does not arise). The model exhibits high computational efficiency due to its discrete nature, which allows to perform almost all calculations on the basis of integer arithmetic.

In the systems under consideration, model objects of the two types are present: polymer chains with a given number of monomeric units ($N_p = 16$) and colloidal particles, which are actually similar but shorter chains of two monomeric units (i.e., dimers with $N_d = 2$). To identify these objects, in the subsequent text we use the subscripts p and d, respectively. Evidently, the chosen representation of a polymer and a small particle is rather arbitrary. However, it should be emphasized that only the relation between the sizes of the polymer chain and the colloidal particle is significant for the problems under consideration (see below).

As is mentioned above, three 2d systems are studied. The base system contains n_p chains and n_d colloidal particles placed in a square $L \times L$ cell with periodic boundary conditions. The same cell is used for two reference systems. One of the reference systems consists of n_p N_p-unit chains; the other, of n_d colloidal particles (dimers). The average partial number densities of the polymer ρ_p and colloidal particles ρ_d always coincide for the base and reference systems. Note that in our 2d model the partial volume fractions of the components are $\Phi = \Omega\rho$, where $\Omega = (2\sigma)^2$ is the area per one monomer, and $\rho = nN/L^2$. Note also that although the base and reference systems are binary or

one-component, we can consider them as ternary or binary systems, respectively, because at $\Phi_p + \Phi_d < 1$ vacant lattice sites play a role of low-molecular-weight solvent.

Now, let us consider the energy effects. Within the framework of classical lattice theories (the Flory–Huggins-type theories [64]), for a homogeneous polymer solution the effect of solvent on macromolecular conformations is characterized by the parameter χ, which is the difference of the polymer–solvent interaction energy (ε_{ps}) and the half sum of the polymer–polymer and solvent–solvent interaction energies (ε_{pp} and ε_{ss}, respectively):

$$\chi = \frac{\tilde{z}}{k_B T}\left[\varepsilon_{ps} - \tfrac{1}{2}\left(\varepsilon_{pp} + \varepsilon_{ss}\right)\right], \tag{1}$$

where k_B is the Boltzmann constant and $\tilde{z}$ is the effective lattice coordination number. In the same manner as in our model, it is assumed that the role of a solvent (s) belongs to vacant lattice sites. Good solvents have low values of χ; poor solvents have high values of χ, a special case is $\chi = 1/2$, which corresponds to Θ conditions. In the computer model, the analog of χ is the parameter ε_{pp} that governs the interaction between any two chain monomers occupying the neighboring lattice sites at a distance from 2 to $8^{1/2}$ lattice units; that is the maximum number of monomers with which a given monomer may interact is equal to 16. At $\varepsilon_{pp} = 0$, the athermal conditions are reproduced, i.e. the only type of interaction between chain monomers is the steric repulsion due to mutual impenetrability of monomers. At $\varepsilon_{pp} < 0$, attraction between monomeric units occurs, i.e., the solvent quality degrades. In our computer model, the same role belongs to the parameter ε_{dd} that describes the interaction between the monomeric units of colloidal particles. Finally, the parameter ε_{pd} describes the surface affinity (i.e., adsorption) of the polymer component to the colloidal particles. Evidently, adsorption is possible only when $\varepsilon_{pd} < 0$. In the subsequent text, we give all energy parameters in the units of $k_B T$.

The displacement of a randomly chosen monomeric unit α (that belongs to a polymer chain or a colloidal particle) from the old position $\mathbf{r}_\alpha$ to the new one $\mathbf{r}'_\alpha$ is performed using the standard Metropolis procedure [61] with the probability

$$\mathscr{P}(\mathbf{r}_\alpha \to \mathbf{r}'_\alpha) = \min\{1, \exp(U - U')\}, \tag{2}$$

where

$$U = \varepsilon_{pp} \cdot z_{pp}(\mathbf{r}_\alpha) + \varepsilon_{dd} \cdot z_{dd}(\mathbf{r}_\alpha) + \varepsilon_{pd} \cdot z_{pd}(\mathbf{r}_\alpha), \tag{3a}$$

$$U' = \varepsilon_{pp} \cdot z_{pp}(\mathbf{r}'_\alpha) + \varepsilon_{dd} \cdot z_{dd}(\mathbf{r}'_\alpha) + \varepsilon_{pd} \cdot z_{pd}(\mathbf{r}'_\alpha) \tag{3b}$$

and $z_{ij}(\mathbf{r}_\alpha)$ and $z_{ij}(\mathbf{r}'_\alpha)$ are the numbers of the corresponding contacts $i \ldots j$ (i, j = p, d) in the positions $\mathbf{r}_\alpha$ and $\mathbf{r}'_\alpha$. Apparently, $\mathscr{P} = 0$ if the excluded-volume or chain-connectivity constraints are not satisfied. The "simulation clock" is updated by one time unit independently of whether the move is accepted or rejected. As usual, the conventional time t is measured in Monte Carlo steps (MCS), i.e., the number of elementary moves per monomeric unit of the system. The sufficient accuracy of calculations is achieved when the observed values are averaged over the stationary part of a trajectory of $t \sim 10^6$ MCS, i.e., over $\sim 10^6$ nN configurations.

The three-dimensional system

In the case of 3d simulation, we employ the standard bond-fluctuation model that is described in the paper of Deutsch and Binder [63]. Similar to the 2d system, colloidal particles are modeled by dimers ($N_d = 2$). The volume fraction of the particles is given by $\Phi_d = (2\sigma)^3 n_d N_d / L^3$. The volume fraction of polymer chains, $\Phi_p = (2\sigma)^3 n_p N_p / L^3$, is the same as for the 2d system; the length of the chains, however, is $N_p = 64$. The maximum number of different monomers with which a given monomer may interact is 98. This corresponds to the "interaction distance" belonging to the range $2\sigma \le r \le \sqrt{12\sigma}$. We introduce interaction energies ε_{pp}, ε_{dd}, and ε_{pd} between monomers belonging to different types of species. As a rule, we consider the athermal conditions when energies between monomers of the same kind are set equal to zero, $\varepsilon_{pp} = \varepsilon_{dd} = 0$. In this case, it is convenient to express the characteristics of a system as functions of the reduced temperature $T = 1/|\varepsilon_{pd}|$. Initial states were prepared by placing all the species within the $64 \times 64 \times 64$ cube with periodic boundary conditions and then were annealed for $\sim 5 \times 10^5$ MC steps. Averages were then calculated from the following 5×10^5–10^6 MCS.

Let us give some comments to the assumptions adopted in the models under study. As has been mentioned in the Introduction, we are interested in the consideration of the interaction between flexible polymer chains and very small particles with a size of the order of the Kuhn segment length A of a chain. First, let us compare spatial scales of the model and real systems. To do this, we must clarify the notation "polymer segment". The model under consideration is a freely jointed chain with arbitary bond angles and fluctuating bond lengths. In such a chain, each monomer is actually a statistical segment. This corresponds to approximately 10 monomeric units of a real flexible polymer chain. The prototype of our model could be the system studied experimentally by Cabane and Duplessix [5–8] using small-angle neutron scattering, namely a semidilute solution of poly(ethylene oxide) (PEO) containing micelles of sodium dodecyl sulfate (SDS) molecules. Using the results of ref. [8], we can find estimations for the characteristic sizes of colloidal particles, σ_d and chain monomer units, σ_p. The average size of the micelles is about 2 nm [8].

The typical size of the statistical segment of flexible polymers (including PEO) is about 1 nm [65]. Therefore, an estimation for a characteristic length scale σ_p is ≈ 1 nm. Since in our case a chain monomer is equivalent to the statistical segment, we have $\sigma_d/\sigma_p \approx 2$. Some other works also report the studies of polymer-containing colloid systems consisting of very small (nanometric) particles. For example, Kabanov and coworkers [66, 67] examined the interaction of microparticles of globular protein (serum albumin with $\sigma_d \approx 2$–3 nm) with quaternized poly(4 -vinylpyridine). In ref. [34], formation of polycomplexes containing colloidal gold particles (particle size of ≈ 5 nm) and poly(2-vinylpyridine) or poly(4 -vinylpyridine) is reported. Spalla and Cabane [12] studied interaction between nanometric particles (crystallites of cerium oxide (ceria) with average diameter $\sigma_d = 6$ nm) and poly(acrylamide) chains with $A \approx 2$ nm. Thus, we can conclude that the relation between the characteristic sizes of our model colloidal particle and the monomeric unit of lattice polymer chains is quite reasonable. As for the chain lengths N_p studied in the present computer simulation, the main condition for the choice of a sufficiently large value for N_p is the inequality $R \gg \sigma_d$, where R is the characteristic chain size. In all the cases considered here this condition is fulfilled.

Second, it is necessary to explain the approximation accepted for interactions in the model system. The considered range of variation of the adsorption energy ε_{pd} includes the values typical for real systems. For example, according to the experimental data [8], the segment adsorption energy for PEO on a micellar surface is $\sim 0.3\, k_B T$. Taking into account the above-mentioned relation between the number of monomeric units in the model and a real system, one can conclude that this value is reproduced at $|\varepsilon_{pd}| \approx 0.3$–0.6 for our 3d model (see also ref. [57]). It is well-known that the most common forces stabilizing disperse systems are electrostatic repulsive interactions [1, 2]. Note, however, that in the case of extremely small (nanometric) particles the corresponding potential barriers are low, since each particle carries a small number of effective charges. For example, for the water dispersion of ceria particles Spalla and Cabane [12] found that the net charge, z^{eff}, is 17 electron charges per particle. Also, they estimated the range σ_r of electrostatic repulsion as a function of pH and showed that the value of σ_r is rather short: $\sigma_r/\sigma_d \approx 2$–4 at pH $\in (1.7, 3.4)$.

Correlation functions

The main structural characteristics used in our calculations are the pair correlation functions, $g(r)$, and the collective static structure factors, $S(q)$.

Let us define the density–density correlation function

$$g(\mathbf{r}) = \frac{\langle \rho(0) \cdot \rho(\mathbf{r}) \rangle}{\rho^2}, \tag{4}$$

where ρ is the average number density of interaction sites (i.e., monomeric units belonging to polymer chains or colloidal particles) and $\rho(\mathbf{r})$ is the local number density at point $\mathbf{r}$. For an isotropic system, the density–density correlation function is equivalent to the radial density distribution function

$$g(r) = \frac{\langle \rho(r) \rangle}{\rho}, \tag{5}$$

where $\langle \rho(r) \rangle$ is the average local density of the interaction site belonging to a given type of species. For the lattice systems under consideration, $r \equiv |\mathbf{r}_\alpha - \mathbf{r}_\beta|$ is the distance between two occupied lattice sites α and β.

For each configuration of N occupied sites, there are $N(N-1)/2$ distances $r_{\alpha\beta} = |\mathbf{r}_\alpha - \mathbf{r}_\beta|$ between these sites. Let us construct the histogram $h(r_i)$ for the distances $r_{\alpha\beta}$. In other words, $h(r_i)$ is the number of distances $r_{\alpha\beta}$ equal to $r_i = i\Delta r$ where $i = 1, 2, 3, \ldots$, and Δr is the histogram step. To calculate $g(r)$ in a discrete regular space, we must take into account that each layer of thickness Δr at a distance of r_i from the origin has a definite number of positions $k(r_i)$.

Therefore, for each layer i, normalization must be by $k(r_i)$ and not by the layer volume (area). Then, for a certain configuration the "instantaneous" radial distribution function is

$$g_t(r) = 2L^2 h(r_i)/N^2 k(r_i) \tag{6}$$

with the normalization factor determined by the condition

$$\rho \sum_i g_t(r_i)\, k(r_i) = N - 1 . \tag{7}$$

Averaging of equilibrium conformations gives the expression

$$g(r) = 2L^2 \langle h(r_i) \rangle / N^2 k(r_i) . \tag{8}$$

The static structure factor is given by

$$S(q) = \frac{1}{N} \sum_{\alpha=1}^{N} \sum_{\beta=1}^{N} \langle \exp[\mathrm{i}\mathbf{q} \cdot (\mathbf{r}_\alpha - \mathbf{r}_\beta)] \rangle , \tag{9}$$

where $\mathbf{q}$ is the wave vector, $\mathbf{r}_\alpha$ is the position vector of occupied lattice site α in a given configuration, $\langle \cdot \rangle$ means an ensemble average, and $\mathrm{i} = \sqrt{-1}$. Calulation of $S(q)$ for a lattice model requires some comments. Because the lattice is discrete and the Monte Carlo cell is finite, there are special constraints on the number of possible values of

$q = |\mathbf{q}|$ and $r_{\alpha\beta}$. For example, the minimum q is $2\pi/L$, and the set of possible values of q is defined by the finite number of different wave vectors compatible with the L^d reciprocal Bravais lattice. Because we are interested in the behavior of $S(q)$ at small q, which describes the large-scale arrangement in the system, it is evident that the lattice sizes must be as large as possible. Actually, as was mentioned previously, this condition can be achieved only for two-dimensional systems.

Using $g(r)$, we can define the following measure of effective site–site interaction:

$$B = \frac{1}{2}\int_{\mathbf{r}} d\mathbf{r}\,(1 - e^{\Psi/k_B T}) , \tag{10}$$

where Ψ is the effective pair potential (i.e., potential of mean force) which is expressed in terms of $g(r)$ as

$$\Psi = -k_B T \ln [g(r)] . \tag{11}$$

Actually, B is the effective monomeric second virial coefficient. Positive values of B correspond to repulsion, negative ones describe attraction, and at $B = 0$ we have a system of effectively noninteracting particles (i.e., the spatial distribution of the particles is the same as in a perfect gas).

In addition to the effective monomeric second virial coefficient, we can define the isothermal compressibility for a given subsystem

$$\chi_T = V^{-1}(\partial V/\partial P)_T = (k_B T\rho)^{-1} + (4\pi/k_B T)\int dr\, r^2[g(r) - 1] . \tag{12}$$

On the other hand, the reduced isothermal compressibility, $\chi^* = k_B T \rho \chi_T$, is given by

$$\chi^* = \lim_{q\to 0}[S(q)] . \tag{13}$$

At $\chi^* < 1$, the repulsive interaction prevails under the given conditions; at $\chi^* > 1$, the effective attraction dominates; at $\chi^* = 1$ (or $B = 0$), the balance of the attractive and repulsive forces is established and the system behaves as an ideal one. Equations (10)–(13) give a simple relation between the value of B and χ_T.

Results of the simulations

Chain sizes

We characterize the size of a chain by its mean-square gyration radius

$$\langle R_g^2\rangle = \frac{1}{N_p}\sum_{\alpha=1}^{N_p}\langle(\mathbf{r}_\alpha - \mathbf{r}_0)^2\rangle , \tag{14}$$

where $\mathbf{r}_\alpha$ is the position vector of the αth monomeric unit, $\mathbf{r}_0 = (1/N_p)\sum_\alpha \mathbf{r}_\alpha$ is the position vector of the center of mass of the chain, and the angle brackets $\langle\cdot\rangle$ denote averaging over all configurations and all n_p chains of the systems.

First of all, we must choose a reference state for the energy parameter ε_{pp} in a way convenient for subsequent analysis. As such a state, we choose the state corresponding to the value of $\varepsilon_{pp} = \varepsilon_\Theta$, at which a chain of a given length N_p is in Θ conditions. i.e., its average size is the same as for an ideal chain without excluded volume interactions. To find the corresponding unperturbed value $\langle R_g^2\rangle_\Theta$, we must set $\varepsilon_{pp} = 0$ and exclude all steric constraints, but retain the constraints imposed on the bond lengths. Under these conditions, Monte Carlo simulation performed for $N_p = 16$ gives $\langle R_g^2\rangle_\Theta = (24.7 \pm 0.01)\sigma^2$ for the 2d system.

Now, let us consider the dependence of $\langle R_g^2\rangle$ on ε_{pp} for a system of self-avoiding chains. Figure 2 presents the results of calculations performed for the 2d system. It can be seen that the polymer coils contract with decreasing ε_{pp}. The condition $\langle R_g^2\rangle = \langle R_g^2\rangle_\Theta$ is fulfilled at $\varepsilon_{pp} = \varepsilon_\Theta \approx -0.8$. This means that in the 2d system under consideration the conditions of a good solvent are realized at $\varepsilon_{pp} > -0.8$; at $\varepsilon_{pp} \le -0.8$, we have a poor solvent.

Let us consider the effect of the polymer–particle attraction on the behavior of the 2d base system. To do this, we set $\varepsilon_{pp} = 1$, which provides strong swelling of polymer coils. For the parameter ε_{dd} that characterizes the interaction between model colloidal particles, we also choose the value $\varepsilon_{dd} = 1$. Figure 2 shows the chain size as a function of the adsorption energy ε_{pd}. As seen, in the absence of adsorption, i.e., at $\varepsilon_{pd} = 0$ the values of $\langle R_g^2\rangle$ obtained at the same values of ε_{pp} almost coincide for the reference and base systems. The value of $\langle R_g^2\rangle$ exhibits weak variation in the region $\varepsilon_{pd} \ge -1.25$. This result is in a good agreement with the theoretical predictions [44]. However, at stronger adsorption of chains on particles, considerable decrease in average chain sizes is observed. We can say that the adsorption induces effective intramolecular attraction of the polymer segments. The attraction caused by chain binding with the particles results in approximately the same behavior of $\langle R_g^2\rangle$ as in the case when the adsorption is absent but the solvent is poor (Fig. 2, curve 1). Nevertheless, we note that under the conditions studied, the value of $\langle R_g^2\rangle$ remains larger than $\langle R_g^2\rangle_\Theta$. Therefore, although considerable contraction of polymeric coils occurs, still the coils are swollen. In the vicinity of the Θ point, the situation is different (Fig. 2, curve 3). At $\varepsilon_{pp} = -0.5$, in the absence of adsorption $\langle R_g^2\rangle$ is still larger than $\langle R_g^2\rangle_\Theta$. However, if adsorption is sufficiently strong, the conditions of a poor solvent are actually realized for polymer chains. In this case, in a macroscopic system the solubility of the polymer component must decrease and the polymer must

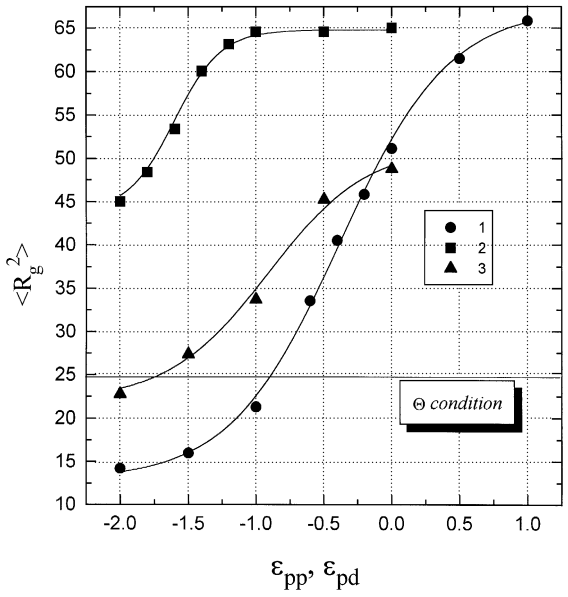

Fig. 2 The mean-square gyration radius $\langle R_g^2 \rangle$ for a polymer chain as a function of the polymer-polymer or polymer–particle interaction energies (ε_{pp} and ε_{pd}, respectively): curve 1, $\langle R_g^2 \rangle$ against ε_{pp} for the reference one-component polymer system (the horizontal line corresponds to the Θ conditions); curve 2, $\langle R_g^2 \rangle$ against ε_{pd} at $\varepsilon_{dd} = \varepsilon_{pp} = 1$ for the 2d base system; curve 3, $\langle R_g^2 \rangle$ against ε_{pd} at $\varepsilon_{pp} = -0.5$ and $\varepsilon_{dd} = 1$ for the 2d base system. The cell size is 128×128. Both the systems contain $n_p = 32$ chains of $N_p = 16$ segments. The base system contains also $n_d = 128$ colloidal particles (with $N_d = 2$)

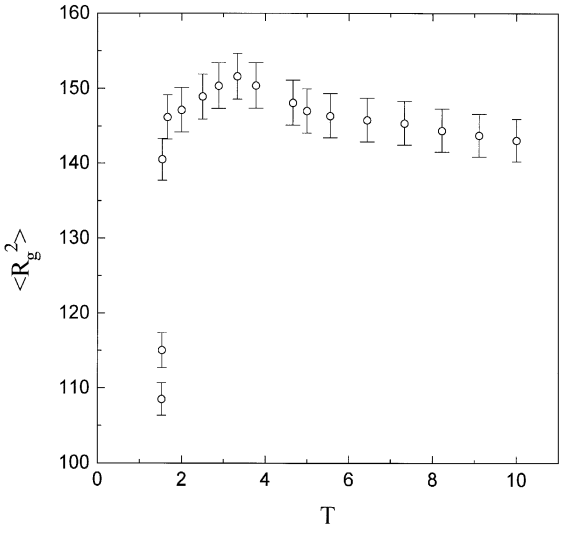

Fig. 3 $\langle R_g^2 \rangle$ vs. T for the 3d system consisting of $n_d = 512$ colloidal particles and $n_p = 64$. 64-unit chains placed in the cubic cell with $L = 64$. Notice the maximum near $T = 3$

precipitate from the solution with the capture of the colloidal particles. This behavior is often observed experimentally [1, 2].

Now, we consider the mean chain dimensions for the 3d system. In this case we set the volume fraction of polymer $\Phi_p = 0.125$, as for the 2d system. This value of Φ_p corresponds to a semidilute polymer solution. The volume fraction of colloidal particles we set $\Phi_d = 1/64$. For the given Φ_p and Φ_d there are 5120 particles in a periodic cubic cell with the edge length $L = 64$. Figure 3 shows $\langle R_g^2 \rangle$ as a function of the reduced temperature $T = 1/|\varepsilon_{pd}|$ at $\varepsilon_{pp} = \varepsilon_{dd} = 0$. It is seen that the chains become more compact as T is decreased. Generally, the same behavior is observed for the 2d system. In the region $3 \leq T \leq 6$, however, a small increase in $\langle R_g^2 \rangle$ occurs. Though this effect is rather small it is possible to assert that, when the adsorption of the polymer on particles is not very strong, some extra swelling of coils takes place, as compared with purely athermal system. We recall the theoretical prediction of such a swelling made by Klimov and Khokhlov [44] for the adsorption of chains on the surface of spatially fixed colloidal particles. At $T \leq 2$, i.e., under sufficiently strong adsorption, the chain dimension drops sharply, as it is well seen in Fig. 3.

Thus, our computer simulation predicts the compression of the chains when adsorption is strong enough.

It should be noted that reversible adsorption of small particles or low-molecular-weight compounds (ligands) on monomeric units of a single polymer chain is a well known phenomenon in physics and chemistry of polymers and biopolymers [68–70]. Due to the reversibility of adsorption, such polymer–particle complexes have a number of various specific properties. One of the most interesting of these properties is the possibility of intramolecular phase separation within the chain. The detailed investigation of this phenomenon has been performed by Dormidontova et al. [71] for a single polymer chain in dilute solution. Using a Flory-type interpolation theory they showed that, in the course of the intramolecular phase separation under certain conditions, spatial structure of the chain is affected. As adsorption increases the adsorbed particles tend to concentrate on some section of the chain with simultaneous contraction (globularization) of this section, while the other part of the chain including only a few monomeric units with adsorbed particles remain in the state of a coil. As a result, for an infinitely long chain with statistically uniform distribution of adsorbed particles, the macromolecular collapse occurs (as a standard coil-globule transition [72]). It seems that a similar adsorption-mediated contraction of coils is observed for our short chains in semidilute solution. Briefly, it is explained by the fact that a chain segment "stuck" to the surface of a colloidal particle attracts the neighboring sections of the same chain. In a sense we can consider the particles as mobile junctions. Of course, to investigate the phase behavior of

the system it would be desirable to perform grand-canonical or semi-grand-canonical numerical simulations [73, 74] taking into account the variable concentrations of both the polymer and the colloids.

Effective interaction between the colloidal particles

Let us now consider the effect of adsorption on the interaction between the colloidal particles. As a measure of this interaction, we use the effective monomeric second virial coefficient B calculated for the colloidal particles.

Note that the calculation procedure described above (see correlation functions Section) always leads to B values including the contribution of monomeric units binding in dimers, because this contribution is not eliminated from $g(r)$. However, it follows from our calculations that this contribution is almost independent of any parameters of the system. To eliminate this model-dependent contribution, it is convenient to consider the normalize value $B^* = (B - B_{ref})/B_{ref}$, where B_{ref} describes some reference configuration (see below).

Figure 4 presents the values of B^* calculated for the 2d base system and for the 2d reference system consisting only of colloidal particles. In the first case, the energy parameters ε_{pp} and ε_{dd} were fixed ($\varepsilon_{pp} = \varepsilon_{dd} = 1$) and B^* is considered as a function of the adsorption energy ε_{pd}. In the second case, we have a single energy parameter ε_{dd}. In the calculations of B^*, we use the following reference states: (i) $\varepsilon_{pd} = 0$ (at $\varepsilon_{pp} = \varepsilon_{dd} = 1$) and (ii) $\varepsilon_{dd} = 1$.

As seen from Fig. 4, with the increasing attraction between the particles, B^* decreases. Apparently, it must be so in the case of ordinary aggregation. However, for the base system with repelling particles (at $\varepsilon_{dd} = 1$) we also observe a fast decrease of B^*. In this case, the decrease in B is due to the effect of the polymer chains adsorbed on the particles and but not due to the attraction between the colloidal particles.

It should be noted that the values of B observed for the 2d base system at $\varepsilon_{pd} = -1$ slightly overcomes the same value obtained for the case without adsorption (i.e., for $\varepsilon_{pd} = 0$). This effect, however, is rather weak; it lies within the statistical errors of calculations. Nevertheless, as we will see later there is a well-pronounced increase in the B value for the 3d system.

Let us now consider the results obtained for the 3d system. In this case, in addition to the effective second virial coefficient we discuss the isothermal compressibility for the subsystem of colloidal particles, χ_T (see Eq. (12)).

The ratio $B(T)/B(\infty)$ as a function of temperature is presented in Fig. 5 for the 3d system at $\varepsilon_{pp} = \varepsilon_{dd} = 0$, $\varepsilon_{pd} = -1$, $\Phi_p = 0.125$, and $\Phi_d = 1/64$. We find that the value of B exhibits a nontrivial behavior. If the high-

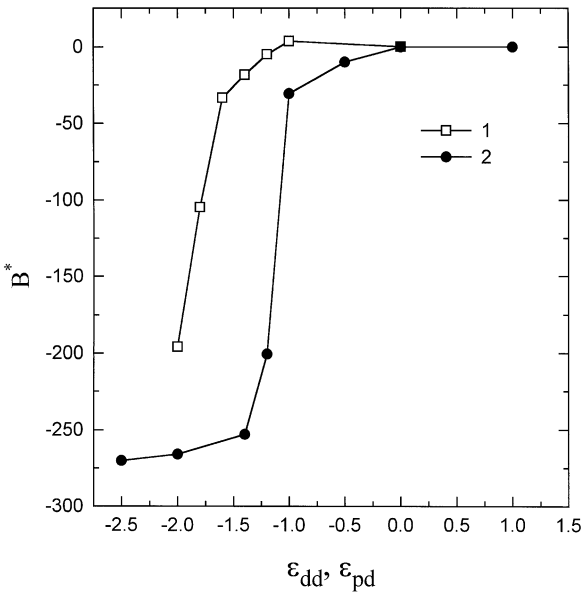

Fig. 4 The value of B^* as a function of ε: curve 1, B^* as a function of ε_{pd} for the 2d base binary system ($L = 128$, $n_d = 128$, $n_p = 32$, $N_p = 16$, $\varepsilon_{dd} = \varepsilon_{pp} = 1$); curve 2, B^* against ε_{dd} for the 2d reference one-component system ($L = 128$, $n_d = 128$)

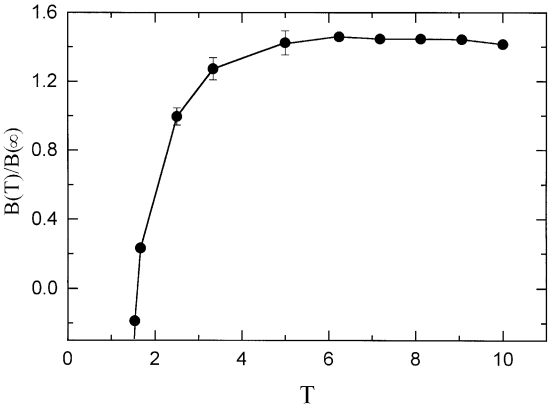

Fig. 5 The normalized value of $B(T)/B(\infty)$ vs. T for the 3d system consisting of $n_d = 512$ colloidal particles and $n_p = 64$. 64-unit chains places in the cubic cell with $L = 64$

temperature limit ($T \to \infty$ or $\varepsilon_{pd} = 0$) is taken as a reference point, then with decreasing temperature (i.e., with strengthening of adsorption) the value of B first increases and then begins to drop rapidly; on the contrary, the value of χ_T first decreases and then grows. In both the cases, the temperature dependencies have an extreme, exhibit relatively slow variation at high T, and undergo drastic changes at low T. Let us consider what happens in these temperature regions.

By strengthening the adsorption of chains on particles, the formed polymer coat begins to screen the particle

surface and, thus, makes their contact with each other difficult. In other words, when adsorption is sufficiently strong, the colloidal particles are drawn apart and the corresponding interparticle distances redistribute in space. As a result of such spatial redistribution of the particle density in the system, the function $B(T)$ accounting for the effective medium-induced interaction between particles increases with decreasing T. One can say that in this case we observe "repulsion through attraction". It is easy to understand that the same reason must result in the decrease of the compressibility χ_T. Thus, there is a wide temperature region characterized by relatively small compressibility of the subsystem of particles. In this region the repulsive forces prevail in the effective medium-induced interaction between particles. Using the terms of colloid science we can say that, in the case of weak adsorption, the polymer additives increase the aggregation stability, i.e., the polymer plays the role of a stabilizer of the dispersion.

As seen from Fig. 5, at a certain temperature $T = T_1$ (which generally depends on the system parameters) we have: $B(T_1)/B(\infty) = 1$ (or $\chi_{T_1}/\chi_\infty = 1$). Under these conditions, the system behaves similar to the case without adsorption. Further decrease in T leads to rapid variation in $B(T)$ and χ_T. At T less than some threshold value $T^* \approx 1.55$, the value of B becomes negative; that is, under these conditions the addition of a polymer results in the mutual attraction of the colloidal particles. Again, speaking about attraction between the particles, we mean not their direct attraction, which is not taken into account in the present calculation, but the effective, polymer-mediated attraction. Therefore, in the binary system under stuedy the collidal particles show a tendency to aggregation at $T \leq 1.55$.

At this point, it is necessary to note that the characteristics discussed above give only an indirect information about aggregation of the particles and reveal only general tendencies of this process. For a more complete description, the direct calculation of average aggregate size is desirable.

Aggregation of the particles

In order to consider the formation of aggregates (clusters), we first need to define what an aggregate is. The standard definition, in the continuous space, implies that each particle is surrounded by an imaginary sphere of a given radius R_c, then an αth particle is considered as belonging to a given aggregate if at least another particle β belonging to the same aggregate lies inside the αth imaginary sphere. The number of particles thus constructed is the instantaneous aggregation number m.

At equilibrium, the aggregation process is characterized by the time-averaged distribution function

$$W(m) = \mathcal{N}(m)/\Sigma_m \mathcal{N}(m) , \tag{15}$$

where $\mathcal{N}(m)$ denotes the mean number of clusters consisting of m particles. Thus, the average aggregation number is

$$\langle m_{av} \rangle = \Sigma_m W(m) m . \tag{16}$$

For our 3d lattice model, we set $R_c^2 = 12\sigma^2$; that is, we assume that two particles are in contact if they are direct or diagonal neighbors on a lattice. In addition to $\langle m_{av} \rangle$, we have calculated the average maximum aggregation number $\langle m_{max} \rangle$ as well as the average number of particle–particle and polymer–particle contacts, $\langle k_{dd} \rangle$ and $\langle k_{pd} \rangle$. It is clear that $\varepsilon_{pd} \langle k_{pd} \rangle$ is simply the total average potential energy of interaction between particles and polymer chains. All the results are presented in Figs. 6–8 for the 3d model.

One can see that the temperature behavior of $\langle m_{av} \rangle$, $\langle m_{max} \rangle$, and $\langle k_{dd} \rangle$ is nonmonotonic: there is a slow decrease at high T and an abrupt, jump-like, growth at low $T < T^*$. The analogous features have been observed for $B(T)$ and χ_T. On the other hand, with the decrease in temperature the value of $\langle k_{pd} \rangle$ always increases showing a rather quick rise near T^*. Thus, the general tendency is that with the strengthening of adsorption the aggregates first destroy partially (at $T > T_1$) and then their sizes begin to grow rapidly (at $T < T^*$). Of course, this type of behavior depends on the interactions involved and other system parameters, but it undoubtedly takes place.

It is interesting to study the kinetics of the formation of the clusters. With that end in view we use a well-equilibrated athermal system ($T = \infty$) which is considered as an initial state. Then this 3d system was abruptly "quenched" to the temperature $T = 1.5$; in other words, the parameter ε_{pd} at some moment was switched from $\varepsilon_{pd} = 0$ to $\varepsilon_{pd} = -\frac{2}{3}$. The time evolution of m_{av} and m_{max} after such "quenching" is presented in Fig. 9. It is seen that $t \leq 10^5$ MCS the initial cluster sizes are approximately the same as in the initial state; then we observe the aggregation of particles. The specific shape of the functions $m_{av}(t)$ and $m_{max}(t)$ is explained by the random contacts of neighboring large aggregates. It is evident that appearing or disappearing of at least one of such contacts changes m_{av} and m_{max} in a jump-like manner. The presence of these large aggregates built from colloidal particles is evident from snapshot pictures (see below).

Thus, we can speak about a special type of aggregation induced by particle binding with polymer molecules. In this sense, the polymer additive plays a role of a destabilizing agent, which decreases the aggregation stability of the disperse phase.

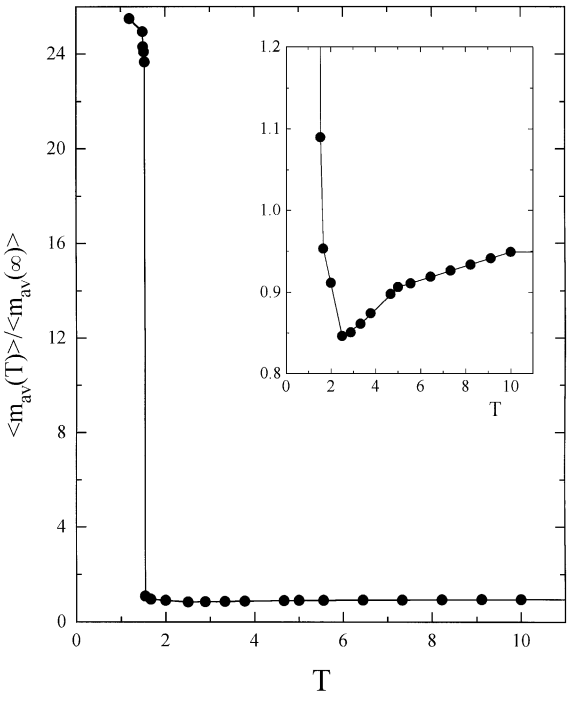

Fig. 6 The normalized value of $\langle m_{av}(T)\rangle/\langle m_{av}(\infty)\rangle$ vs. T for the 3d system consisting of $n_d = 512$ colloidal particles and $n_p = 64$. 64-unit chains placed in the cubic cell with $L = 64$. Notice the minimum near $T = 2.5$

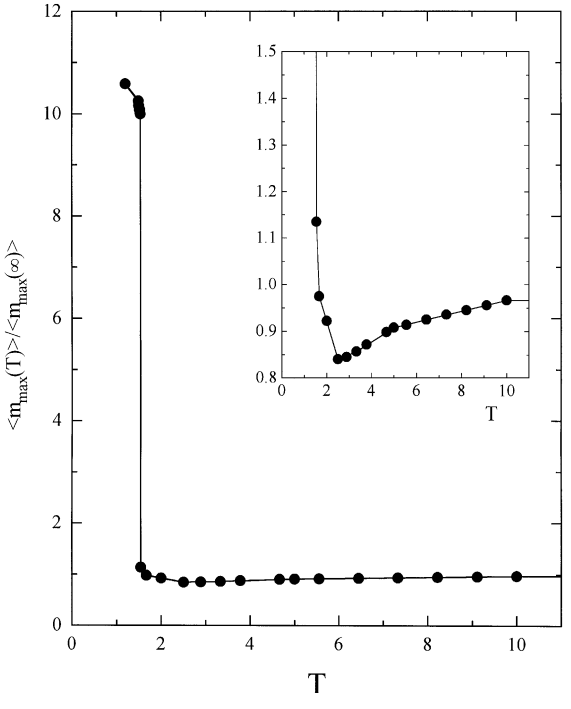

Fig. 7 The normalized value of $\langle m_{max}(T)\rangle/\langle m_{max}(\infty)\rangle$ vs. T for the 3d system consisting of $n_d = 512$ colloidal particles and $n_p = 64$. 64-unit chains placed in the cubic cell with $L = 64$. Notice the minimum near $T = 2.5$

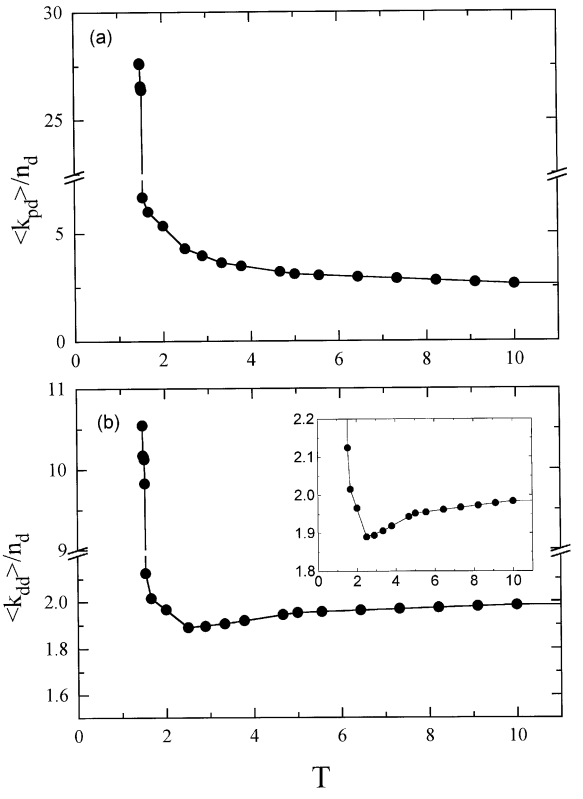

Fig. 8 The normalized value of $\langle k_{pd}\rangle$ and $\langle k_{dd}\rangle$ vs. T for the 3d system consisting of $n_d = 512$ colloidal particles and $n_p = 64$. 64-unit chains placed in the cubic cell with $L = 64$. Notice the minimum near $T = 2.5$ for $\langle k_{dd}\rangle$

Diffusion of the particles

We have calculated the mean square center-of-mass displacement of small particles for the 3d system. Then, self-diffusion coefficients, D, were determined from the Einstein relation:

$$\langle[\mathbf{R}_{cm}(t + t_0) - \mathbf{R}_{cm}(t_0)]^2\rangle = 6Dt\ , \quad t \to \infty\ . \tag{17}$$

The resulting self-diffusion coefficients are plotted vs. T in Fig. 10. It is seen that a dramatic slowing down with decreasing temperature occurs. Beyond all shadow of doubt, such behavior correlates with the avalanche-like aggregation process observed in the system (see Figs. 6–9).

Structure of the system

The structure factor $S(q)$ was obtained for the colloidal particles of the 2d base and reference systems. Figure 11 presents $S(q)$ for the one-component reference system at different values of the energy parameter ε_{dd}. It can be seen that in the absence of attraction between the particles or

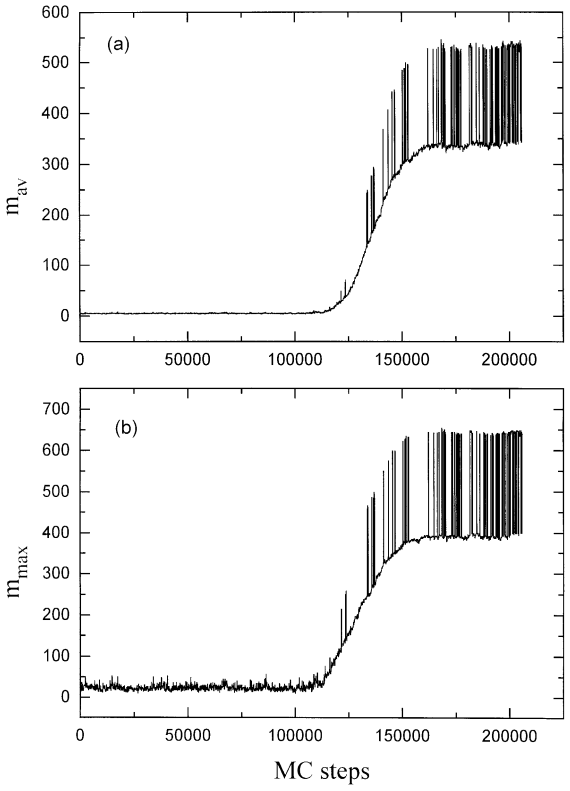

Fig. 9 $\langle m_{av} \rangle$ and $\langle m_{max} \rangle$ vs. time (in unit of MC steps per particle) for the 3d system consisting of $n_d = 512$ colloidal particles and $n_p = 64$. 64-unit chains placed in the cubic cell with $L = 64$ at $T = 1.5$

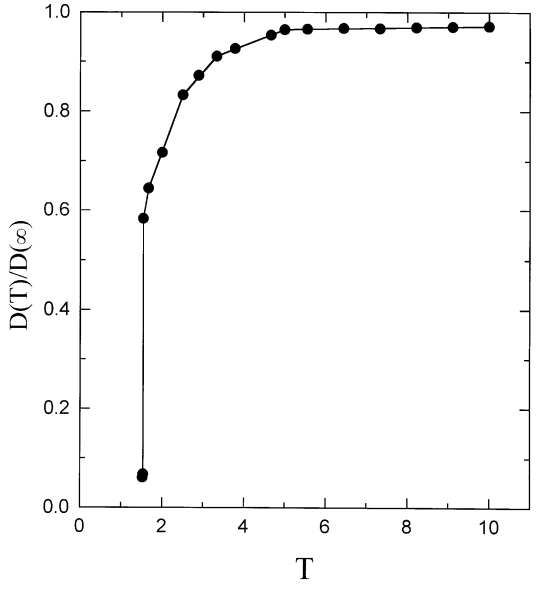

Fig. 10 The normalized self-diffusion coefficient of collodial particles vs. T for the 3d system consisting of $n_d = 512$ colloidal particles and $n_p = 64$. 64-unit chains placed in the cubic cell with $L = 64$

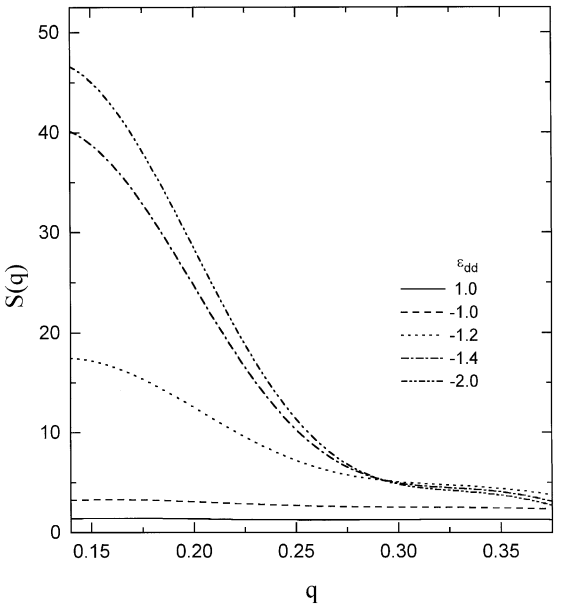

Fig. 11 The static structure factor $S(q)$ for the 2d reference one-component system of the colloidal particles at different energies ε_{dd}. The 128×128 cell contains $n_d = 128$ particles. The value of q is measured in the units of σ^{-1}

when their attraction is weak, $S(q)$ is almost constant at small q. This indicates an approximately homogeneous spatial distribution of the particles. At $\varepsilon_{dd} \leq -1$, the attraction between particles causes their "condensation" and, therefore, the isothermal compressibility of the system increases. The relation (13) makes the increase in $S(q)$ in the region $q \sim 0$ clear. Such a behavior is typical for ordinary condensation phenomena.

Now, let us consider the 2d base binary system. Figure 12 presents $S(q)$ for different values of ε_{pd} at fixed $\varepsilon_{dd} = \varepsilon_{pp} = 1$. It follows from Fig. 12 that in the absence of adsorption, the particle distribution in the binary system is nearly the same as in the one-component system. At $\varepsilon_{pd} \leq -1.2$, structurization of the colloid subsystem occurs. In this case, the particles not only behave in a manner like in ordinary condensation but a quasiregular ordering occurs, which manifests itself as a small-angle peak in the $S(q)$ curve. From the position of the peak (at $q = q_m \approx 0.15$), we can obtain the estimate for the period of the structure formed. It is $r_m = 2\pi/q_m \approx 40\sigma$, which corresponds to about 10 nm for real systems.

Therefore, adsorbing polymer chains can affect the equilibrium spatial distribution of colloidal particles and result in an appearance of a quasiregular structure. As was mentioned in the Introduction, this type of a structure was observed experimentally by small-angle neutron scattering [5–13]. Of course, an important difference of the systems studied in refs. [5–13] and our model must be kept in

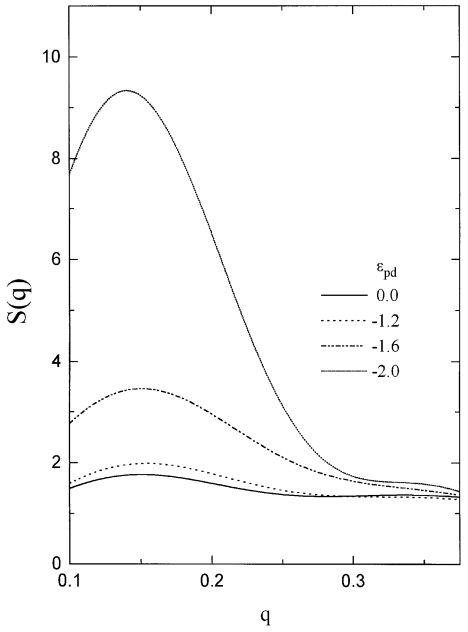

Fig. 12 The static structure factor $S(q)$ for the 2d base binary system at different energies ε_{pd} at $\varepsilon_{dd} = \varepsilon_{pp} = 1$. The 128×128 cell contains $n_d = 128$ particles and $n_p = 32$ chains. The value of q is measured in the units of σ^{-1}

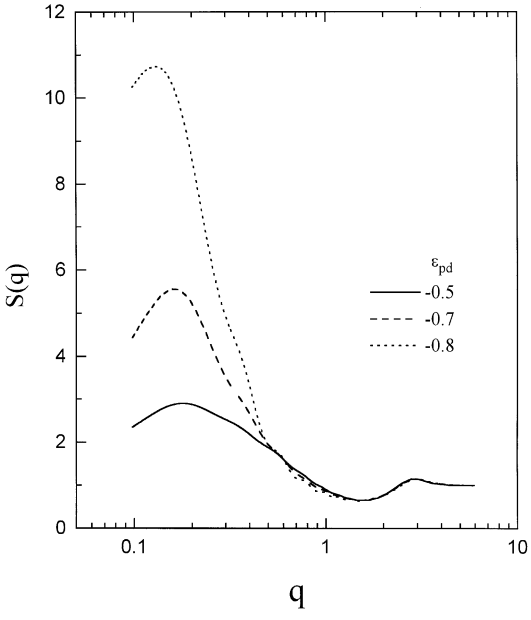

Fig. 13 The static structure factor $S(q)$ for the 3d system at different energies ε_{pd} of polymer–particle interaction. The values of ε_{pp} and ε_{dd} are fixed at $\varepsilon_{pp} = 0$ and $\varepsilon_{dd} = 1$. The 64^3 cell contains $n_d = 512$ particles and $n_p = 64$ 64-unit chains. The value of q is measured in the units of σ^{-1}

mind: in the real experiment [5–13], the colloidal particles (micelles, ceria) are charged so that rather strong mutual repulsion prevents aggregation. Nevertheless, a route to aggregation could be the presence of excess particles in the system [8].

Unfortunately, the calculation of $S(q)$ are less informative for the three-dimensional system, since the Monte Carlo cell is not large enough in this case. This circumstance was noted in the Introduction. That is why we mainly restricted the study of equilibrium structures in the 3d system by visual analysis of typical configurations. Nevertheless, in Figs. 13 and 14 we show the correlation functions $S(q)$ and $g(r)$ calculated for the subsystem of colloidal particles for different values of ε_{pd} at fixed value of the parameter $\varepsilon_{dd} = 1$, i.e., when the short-range interparticle interaction is taken into account. We see that for the 3d system the behavior of $S(q)$ is similar to that observed for the 2d system. At $\varepsilon_{pd} \geq -0.8$, we observe the "small-angle" peak which shifts towards smaller values of q as ε_{pd} is decreased. At very strong adsorption ($\varepsilon_{pd} \leq -0.9$), this peak disappears. In the case of strongly adsorbing macromolecules, the main peculiarity of the pair correlation function $g(r)$ is the appearance of the regime typical for the system in the vicinity of critical conditions when $g(r)$ has a long tail (see Fig. 14). Such long-range correlations reflect a direct analogy with the critical behavior. The picture looks like a low temperature

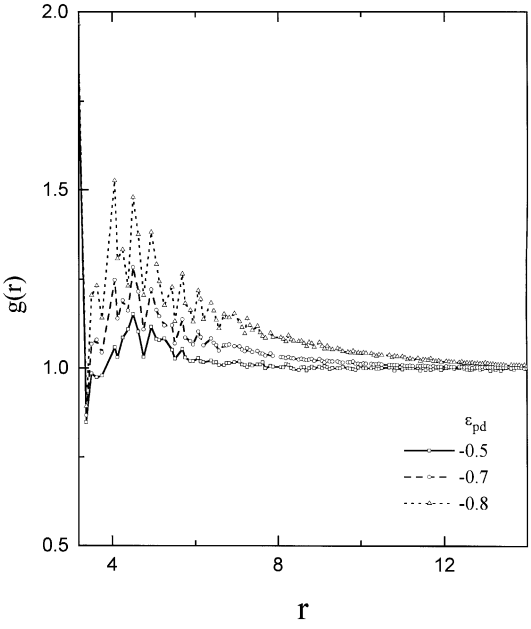

Fig. 14 The pair correlation function $g(r)$ for the 3d system at different energies ε_{pd} of polymer–particle interaction. The values of ε_{pp} and ε_{dd} are fixed at $\varepsilon_{pp} = 0$ and $\varepsilon_{dd} = 1$. The 64^3 cell contains $n_d = 512$ particles and $n_p = 64$. 64-unit chains. The value of r is measured in the units of σ. Note: the saw-like form of the curves is due to lattice nature of the system

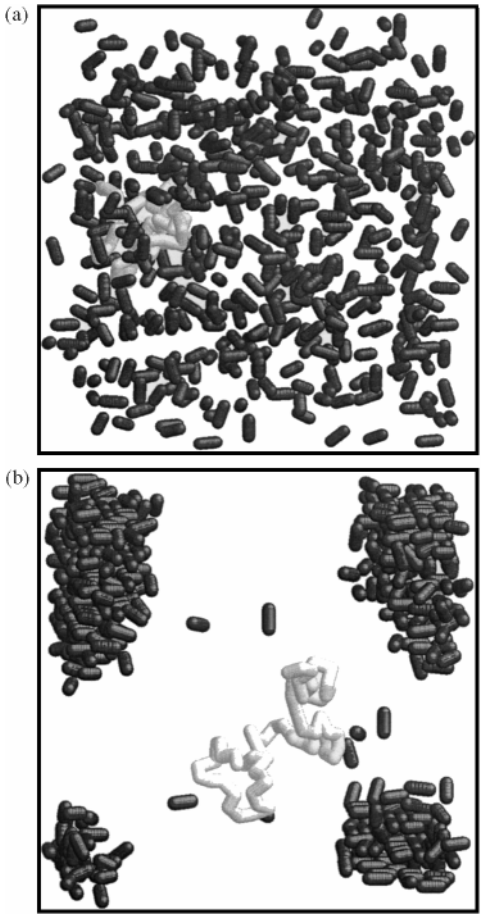

Fig. 15 Snapshot pictures of the 3d system at (a) $T = \infty$ ($\varepsilon_{pd} = 0$) and (b) $T = 1.428$ ($\varepsilon_{pd} = -0.7$). In both the cases, $\varepsilon_{pp} = \varepsilon_{dd} = 0$. The 64^3 cell contains $n_d = 512$ particles and $n_p = 64$. 64-unit chains. The colloidal particles are shown in dark color. For visual clarity, only one chain is presented (in light color)

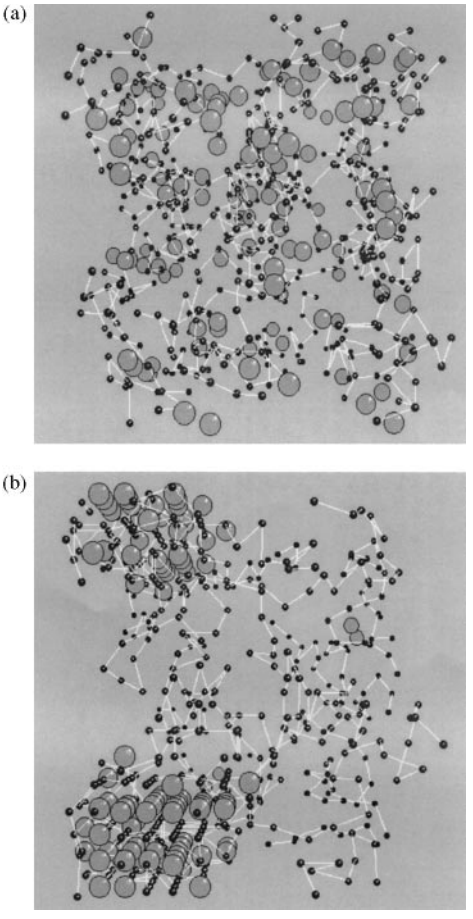

Fig. 16 Snapshot pictures of the 3d system consisting of $n_d = 512$ colloidal particles $n_p = 64$. 64-unit chains placed in the cubic cell with $L = 64$. (a) shows an equilibrated configuration at $T = 1.667$ and $\varepsilon_{dd} = \varepsilon_{pp} = 0$. (b) shows an configuration at $T = 1.5$ and $\varepsilon_{dd} = \varepsilon_{pp} = 0$. Note that some part ($V = 32^3$) of the full 64^3 system is shown only. Larger spheres represent colloidal particles and dark (smaller) spheres are the monomeric units of chains; the sizes of all the spheres are schemetic rather than space filling

"gas–liquid"-type phase separation. We find that this is possible even if the colloid–colloid interaction is strongly repulsive. Apparently, the growth of density–density fluctuations leads to the rapidly increasing osmotic compressibility at small ε_{pd}.

A direct visual analysis of snapshots of the system on the stationary part of its trajectory provides important information concerning the global system architecture and the spatial distribution of particles. Figure 15 presents typical snapshot pictures of the 3d system at $T = \infty$. ($\varepsilon_{pd} = 0$) and $T = 1.428$ ($\varepsilon_{pd} = -0.7$); in both cases, $\varepsilon_{pp} = \varepsilon_{dd} = 0$. In these snapshots we depict the colloidal particles in dark color and, for visual clarity, present only one 64-unit polymer chain (in light color). One can see that without attraction ($\varepsilon_{pd} = 0$) the particles are distributed quite randomly. At strong adsorption ($\varepsilon_{pd} = -0.7$), they aggregate into dense lumps. The structure of the system in the vicinity of the transition temperature, at which the intensive aggregation of particles takes place, is of most interest.

Figure 16 shows two typical instantaneous pictures of the 3d system at equilibrium at $T = 1.667$ and $T = 1.5$ ($\varepsilon_{pp} = \varepsilon_{dd} = 0$). Note that in both the cases some part ($V = 32 \times 32 \times 32$) of the full 64^3 system is shown only. Larger spheres represent colloidal particles and dark (smaller) spheres are the monomeric units of chains; the sizes of all the spheres are schematic rather than space filling. As we can see from Fig. 16, there exists a distinct local nonuniformity of the particle distribution in the pretransition region, where the particles form relatively small clusters. Near the clusters, the density of polymeric units is higher than that averaged over the system. As a result, the polymeric component demonstrates significant density fluctuations. Under similar conditions, we

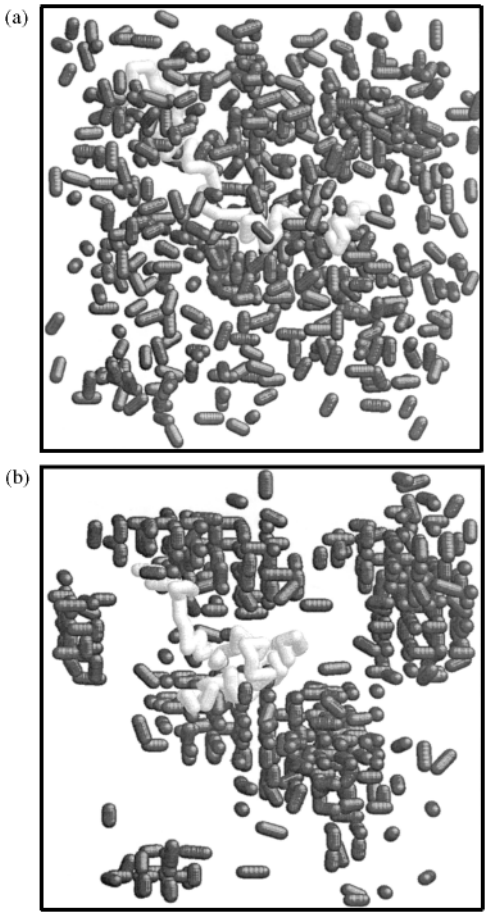

Fig. 17 Snapshot pictures of the 3d system at (a) $\varepsilon_{pd} = -0.8$ and (b) $\varepsilon_{pd} = -0.9$. In both the cases, $\varepsilon_{pp} = 0$ and $\varepsilon_{dd} = 1$. The 64^3 cell contains $n_d = 512$ particles and $n_p = 64$. 64-unit chains. The colloidal particles are shown in dark color. For visual clarity, only one chain is presented (in light color)

have observed the peculiar behavior of the structure factor, $S(q)$ (see Figs. 12 and 13). The sizes of clusters grow as temperature is decreased.

The manipulation of interparticle interactions alone is a convenient way to control the state of the colloidal subsystem. In Fig. 17 we present snapshots obtained for the 3d system in which there is a strong repulsive interaction between the particles ($\varepsilon_{dd} = 1$). We find that in this case the state of the system corresponds to the pretransition region even if the polymer–particle attraction is very strong, $\varepsilon_{pd} = -0.8$. On the other hand, as we saw for the case of $\varepsilon_{dd} = 0$, the particles form large aggregates at $\varepsilon_{pd} \leq -0.65$. However, strongly adsorbing macromolecules may bind particles together, forcing the particles to aggregate into large dense clusters (Fig. 17b).

It is worthwhile to make some more remarks about the structure of equilibrated clusters. The colloidal particles and the chain beads in such clusters pack locally on a binary grid corresponding to a locally crystal-like arrangement, although the packing is distorted on the larger scale by density fluctuations (this is why we use the term "locally crystal-like" to emphasize that we only deal with local order). Clearly, the minimum of the potential energy of this microstructure corresponds to the regularity of the binary grid with an alternating arrangement of the particles and the chain sections. In the limit of strong adsorption (at $T \to 0$) we will have "frozen-in" microstructures; in a sense this situation is similar to the formation of frozen-in microdomains in usual binary mixtures (alloys). Note that, due to the incorporation of the chain sections into the aggregates, the size of the polymer coils reduces (see Fig. 3).

Discussion and conclusions

We have studied two- and three-dimensional model systems that describe the formation of an adsorption complex consisting of polymer chains and small colloidal particles. Although the models are rather simple, they can qualitatively reproduce the phenomena observed experimentally and predict new nontrivial effects.

In particular, we have shown that even in the case of a good solvent the adsorption of polymer on particles can induce effective attraction of polymer chains that results in the contraction of polymer coils. A similar contraction mediated by the reversible adsorption of small particles on a single polymer chain has been predicted theoretically [71] for the case of strong adsorption. On the other hand, our simulations show that there is a wide temperature region, corresponding to the weak or moderate adsorption interaction, where the polymer coils are swollen, as compared to the high-temperature limit. In this region, the repulsive forces prevail in the total polymer-induced interaction between particles. In other words, the polymer plays the role of a stabilizer of colloidal dispersion. The result can be compared with the corresponding theoretical predictions obtained on the basis of the RISM formalism [47]. As was shown in ref. [47], binding of small colloidal particles with flexible-chain macromolecules in a semidilute solution results in a considerable change of properties of both subsystems, as compared to the properties of individual (noninteracting) components. According to ref. [47], the temperature evolution of the functions $B(T)$ and χ_T, describing the behavior of particles, is nonmonotonic: there is a slow increase (decrease) at high T and sharp drop (growth) at low T. We observe the same temperature dependencies of $B(T)$ and χ_T for our lattice models. Further, the theory [15] predicts that with the decrease in temperature, the effective virial coefficient B_{pd}, characterizing the polymer–colloid interaction, always decreases showing a rather quick transition from positive to negative

values. The temperature behavior of the average number of polymer-particle contacts $\langle k_{pd} \rangle$ (see Fig. 8a) can be considered as a confirmation of such a prediction. According to ref. [47], one can locate a particular region of parameters, where compresssibility of the colloidal component is lower than the one observed at the same densities for the system of individual particles., i.e., without polymer additives. This region was called "the region of absolute stability" (see the subregion S in Fig. 1). It seems that the analogous conditions are realized for the 3d computer model when we consider the behavior of the system at the temperature corresponding to the vicinity of lowest values of χ_T or $\langle m \rangle$ (see, e.g., Figs. 6 and 7). One can say that under these conditions we observe "interparticle repulsion through polymer–colloid attraction". Also, the results presented in ref. [15] indicate considerable structural changes due to the formation of specific states characterized by binding together chains and particles at sufficiently low temperature. It was found that the conditions are possible under which both components form well-ordered quasiregular structures exhibiting some features in the scattering functions $S(q)$. This is due to the fact that the saturated adsorption polymer layers surrounding the colloidal particles repel each other in a good solvent through the osmotic pressure of the chain segment. In particular, the appearance of a new maximum in the $S(q)$ curves at certain $q = q^*$ being considerably smaller than the value of q_1 corresponding to the position of the main peak of $S(q)$ for the individual component or for the binary polymer–colloid system at high temperatures was observed. For the colloidal particles, the value of $S(q^*)$ increases with the strengthening of adsorption. We can see the analogous temperature evolution of $S(q)$ in Figs. 12 and 13, taking into account that $T = 1/|\varepsilon|$. Note also that the region of quasiregular structures lie in the vicinity of the curve of critical states of the system where there are large fluctuations of density [47] (see the region D in Fig. 1). As was shown in ref. [47], the structure of the system under the conditions discussed is determined by the packing of adsorption complexes, each consisting of a particle and the neighboring polymer-rich adsorption shell where the local segment density is higher than the average polymer density ρ_p. Packing of such adsorption complexes results in the formation of quasiregular arrays. Naturally, this leads to a considerable nonuniformity in the density distribution which manifests itself as appearance of the "small-angle"peak of $S(q)$ at $q = q^*$. Qualitatively similar behavior is observed in our MC simulations (see Figs. 12 and 13). Position of the q^* peak defines the period of the structure, $r^* = 2\pi/q^*$. For the 2d system considered here we obtain: $r^* \approx 40\sigma$.

Further, the simulations performed in this study have indicated that at sufficiently strong adsorption the particles show a tendency to aggregation. In other words, in this case we observe the polymer-mediated attraction between the colloidal particles which may lead to the coagulation of colloids. This effect has been studied extensively and is well-understood, at least qualitatively [1, 2]. Again, let us compare our results with the predictions of the RISM theory [47]. According to ref. [47], at low temperatures the particle–particle pair correlation function $g(r)$ has a long tail, and the asymptotic decrease of the tail at large r can be described by the Orstein–Zernike relation $\sim r^{-1}\exp(-r/\xi)$, where ξ is the screening length. In the case under discussion such a behavior, well-known for a system being near the critical temperature T_c, is a result of the indirect, polymer-mediated colloid–colloid attraction. (Note that the colloidal particles were modeled in ref. [47] by hard spheres.) The appearance of the long-range particle–particle correlations typical for a system in the vicinity of critical conditions is distinctly seen in Fig. 15. As was shown in ref. [47], at $\rho_d = \text{constant}$ the critical conditions for the colloid subsystem are achieved at some values of the parameters $T = T_c$ and $\rho_p = \rho_p^c$, for which a singularity in compressibility χ_T is observed ($\chi_T \to \infty$ as $T \to T_c$). The same T-dependence of χ_T follows from the data presented in Fig. 5 for the 3d lattice system studied here. Of course, for systems of finite size, χ_T is finite at any T. In the work [47] we failed to study the properties of the system when the condensation of the particles occur, because the integral RISM equations diverge in the vicinity of T_c (the region C in Fig. 1). However, as we have seen, the computer models predict the appearance of large aggregates under these conditions. Hence, we observe the flocculation process in which dissolved macromolecules collect particles of the dispersed phase. This is accompanied by a slowing down of the particle mobility. As for the aggregation mechanism, one could mention the mechanism of aggregation, where particles with saturated adsorption shells would be connected to each other as a result of an excess amount of particles being present in the system. This mechanism has been discussed by Alexander [24]. Recently, using the formalism of the so-called connectedness pair correlation functions, we have studied the aggregation of small colloidal particles interacting with flexible polymer chains [75]. As has been shown in ref. [75], adsorbing flexible-chain macromolecules can function in different ways. When the particle density ρ_d is lower than the percolation threshold density ρ_d^* corresponding to the one-component system of particles, the mean aggregate size first decreases and then begins to grow as the temperature is decreased. This conclusion is supported by our computer simulations. It has also been found [75] that the mean cluster size may become finite and may decrease with decreasing T when ρ_d is slightly greater than ρ_d^*.

In the case of very strong adsorption, we have observed the formation of large compact aggregates with an alternating disposition of the particles and the chain segments, as shown in Figs. 15–17. Note that these structures resemble the semicrystalline structure of the gel-surfactant complexes studied in refs. [76, 77] using synchrotron small angle X-ray scattering.

Acknowledgment Financial support of the E.I. Du Pont de Nemours Company is grateful acknowledged. This work was also supported by the Russian Foundation for Basic Researches (Grant No. 98-03-33348).

References

1. Ottewill RH (1982) In: Goodwin JW (ed) Colloidal Dispersions. Royal Society of Chemistry, London
2. Napper DH (1983) Polymeric Stabilization of Colloidal Dispersion. Academic Press, London
3. Liu SF, Lafuma F, Audebert R (1993) Colloid Polym Sci 272:196
4. Cabane B, Wong K, Lindner D, Lafuma F (1998) J Rheol 43(3), in press
5. Cabane B (1977) J Phys Chem 81:1639
6. Cabane B, Duplessix R (1982) J Phys (France) 43:1529
7. Cabane B, Duplessix R (1985) Colloids and Surfaces 13:19
8. Cabane B, Duplessix R (1987) J Phys (France) 48:651
9. Wong K, Cabane B (1988) J Colloid Interfae Sci 123:466
10. Lafuma F, Wong K, Cabane B (1991) J Colloid Interfae Sci 143:9
11. Wong K, Lixon P, Lafuma F, Lindner P, Aguerre-Charriol O, Cabane B (1992) J Colloid Interfae Sci 153:55
12. Spala O, Cabane B (1993) In: Dubin P, Tong P (eds) Colloid–Polymer Interactions. ACS Symp, Vol 532. ACS, Washington DC, p 35
13. Spala O, Cabane B (1993) Colloid Polym Sci 271:357
14. Asakura S, Oosawa F (1954) J Chem Phys 22:1255; J Polym Sci 33:183 (1958)
15. Fischer EW (1958) Kolloid Z 160:120; Meier DJ (1967) J Phys Chem 71:1861
16. Jäckel K (1964) Kolloid Z 197:143
17. Clayfield EJ, Lumb EC (1966) J Colloid Interface Sci 22:269, 285
18. Lyklema J (1968) Adv Colloid Interface Sci 2:65
19. Hesselink ThF (1971) J Phys Chem 75:65
20. Hesselink ThF, Vriij A, Overbeek FThG (1971) J Phys Chem 75:2094
21. Vincent B (1974) Adv Colloid Interface Sci 4:193
22. Dolan AK, Edwards SF (1974) Proc Roy Soc London 337 A:509
23. Osmond DWJ, Vincent B, Waite FA (1975) Colloid and Polymer Sci 253:676
24. Alexander S (1977) J Phys (France) 38:977
25. Daoud M, de Gennes P-G (1977) J Phys (France) 38:85
26. Joanny JF, Leibler L, de Gennes P-G (1979) J Polym Sci Polym Phys Ed 17:1073; de Gennes P-G (1979) Compt Rend Acad Sci (Paris) 289B:103
27. Gerber PR, Moore MA (1977) Macromolecules 10:476
28. Feigin RI, Napper DH (1980) J Colloid Interface Sci 75:525
29. Klein J, Pincus P (1982) Macromolecules 15:1129
30. Sperry PR (1982) J Colloid Interface Sci 87:375
31. Gast AP, Hall CK, Russel WB (1983) J Colloid Interface Sci 96:251
32. Gast AP, Hall CK, Russel WB (1983) Faraday Discuss Chem Soc 76:189
33. Khalatur PG (1983) Kolloid Zh 45:821, 975; Khalatur PG (1984) Kolloid Zh 46:517
34. Pincus PA, Sandroff CJ, Witten TA (1984) J Phys (France) 45:725
35. Cates DL, Hirtzel CS (1987) J Colloid Interface Sci 120:404
36. Halperin A (1987) Europhys Lett 4:439
37. Vincent B (1987) Colloids Surf 24:269
38. Vincent B, Edwards J, Emmett S, Croot R (1988) Colloids Surf 31:267
39. Fleer GL, Scheutjens JMHM, Cohen Stuart MA (1988) Colloids Surf 31:1
40. Marques CM, Joanny JF (1988) J Phys (France) 49:1103
41. Attard P (1989) J Chem Phys 91:3083
42. Canessa E, Grimson MJ, Silbert M (1989) Molec Phys 67:1153
43. Santore MM, Russel WB, Prud'homme RK (1990) Macromolecules 23:3821
44. Klimov DK, Khokhlov AR (1992) Polymer 33:2177
45. Shaw MR, Thirumalai D (1991) Phys Rev A 44:R4797
46. Yethiraj A, Hall CK, Dickman R (1992) J Colloid Interface Sci 151:102
47. Khalatur PG, Zherenkova LV, Khokhlov AR (1997) J Phys II (France) 7:543
48. Edwards SF, Muthukumar M (1988) J Chem Phys 89:2435
49. Muthukumar M (1989) J Chem Phys 90:4594
50. Honeycutt JD, Thirumalai D (1989) J Chem Phys 90:4542
51. Khokhlov AR, Ternovsky FF, Zheligovskaya EA (1990) Physica A 163:747
52. Ternovsky FF, Nyrkova IA, Khokhlov AR (1992) Physica A 184:342
53. Curro JG, Schweizer KS (1987) J Chem Phys 87:1842
54. Schweizer KS, Curro JG (1994) Adv Polymer Sci 116:319
55. Feigin RI, Napper DH (1980) J Colloid Interface Sci 74:567; 75:525
56. Khalatur PG, Pavlov AS (1983) Polym Sci A 25:1697; Khalatur PG, Pavlov AS (1983) Polym Sci A 25:2599. Khalatur PG (1984) Kolloid Zh 46:294
57. Rozhkov EM, Khalatur PG (1996) Colloid J 58:771; Rozhkov EM, Khalatur PG (1996) Colloid J 58:778
58. Khalatur PG (1996) Computer simulation of polymer systems. In Kuchanov SI (ed) Mathematical Methods in Contemporary Chemistry. Gordon & Breach, New York, pp 487–556
59. Bujan-Nunez MC, Dickinson E (1993) Molec Phys 80:431
60. Bujan-Nunez MC, Dickinson E (1994) J Chem Soc Faraday Trans 90:2737
61. Kremer K (1993) Computer simulation of polymers. In: Allen MP, Tildesley DJ (eds) Computer Simulation in Chemical Physics. Kluwer Academic Publishers, Dordrecht, pp 397–459
62. Karmesin I, Kremer K (1988) Macromolecules 21:2819
63. Deutsch HP, Binder K (1991) J Chem Phys 94:2294
64. Flory PJ (1953) Principles of Polymer Chemistry. Cornell University Press, Ithaca
65. Flory PJ (1969) Statistical Mechanics of Chain Molecules. Wiley, New York
66. Kabanov VA, Evdakov VP, Mustaf'ev MI, Antipina AD (1981) Mol Biol (Moscow) 11:582
67. Ermakova LN, Frolov YuG, Kasaikin VA, Zezin AB, Kabanov VA (1981) Vysokomalek Soed A 23:2328
68. Frank-Kamenetskii MD (1968) Mol Biol (Moscow) 2:408
69. Vedenov AA, Dykhne AM, Frank-Kamenetskii MD (1971) Usp Fiz Nauk 105:479
70. McGhee JD (1976) Biopolymers 15:1345
71. Dormidontova EE, Grosberg AYu, Khokhlov AR (1992) Makromol Chem Theory Simul 1:375
72. Lifshitz IM, Grosberg AYu, Khokhlov AR (1978) Rev Mod Phys 50:683
73. Müller M, Binder K (1994) Comput Phys Commun 84:173
74. Müller M, Binder K (1995) Macromolecules 28:1825
75. Khalatur PG, Zherenkova LV, Khokhlov AR (1997) Physica A 247:205
76. Chu B, Yeh F, Sokolov EL, Starodubtzev SG, Khokhlov AR (1995) Macromolecules 28:8447
77. Yeh F, Sokolov EL, Khokhlov AR, Chu B (1996) J Amer Chem Soc 118:6615